The Rheological and Physical Properties of Linear and Branched Polypropylene Blends

Tara J. McCallum,[1] **Marianna Kontopoulou,**[1] **Chul B. Park,**[2] **Edward B. Muliawan,**[3] **Savvas G. Hatzikiriakos**[3]

[1] *Department of Chemical Engineering, Queen's University, Kingston Ontario, Canada K7L 3N6*

[2] *Department of Mechanical and Industrial Engineering, University of Toronto, Toronto Ontario, Canada M5S 3G8*

[3] *Department of Chemical and Biological Engineering, The University of British Columbia, Vancouver, British Columbia, Canada V6T 1Z3*

The rheological, thermal, and mechanical properties of blends consisting of a linear high melt flow rate polypropylene (PP) and two branched PPs are characterized in detail. Blends containing branched PPs display evidence of miscibility in the melt state and exhibit high melt elasticity together with significant strain hardening in extensional deformation while retaining good flow properties. Out of the two blend systems examined the blends containing linear and branched PPs with similar melt flow rates have better mechanical properties, higher crystallization temperatures, and higher crystallinities. POLYM. ENG. SCI., 47:1133–1140, 2007. © 2007 Society of Plastics Engineers

INTRODUCTION

Polypropylene (PP) is widely used in many processing applications, including extrusion and injection molding. However, PP melts generally do not exhibit the strain hardening behavior necessary for processes that require high melt strength, such as foaming, cast and blown film processing, blow molding, and thermoforming.

With the development and commercial availability of high melt strength long chain branched PPs, new applications have become possible in foaming [1–3] as well as thermoforming [4]. Nevertheless, the cost of branched PPs has deterred their widespread use in industrial operations. The creation of blends of linear and branched PP has the potential to yield new and enhanced materials at a fraction of the cost.

The performance of these blends in foam processing, and in extrusion foaming in particular, is of significant interest. Various studies have indicated that increasing the branched PP content in linear/branched PP blends improves the foaming behavior of conventional PP and results in a higher cell density [5, 6]. Conversely, high-branched PP loadings have resulted in substandard foamability [1]. The addition of branches may also compromise certain mechanical properties, such as strain at break [4]. Therefore, to obtain favorable foaming conditions while maintaining satisfactory mechanical properties, an optimal content of branched PP must be determined. Recent efforts have shown that a peak in cell concentration occurs when 25 wt% branched PP is added to linear PP [7].

It is well known that the presence of branching generally affects the physical properties of polyolefins. As extensive investigations have shown, the phase behavior of polyethylene blends depends heavily on the presence of short or long chain branching [8–15]. Elongational properties have been documented primarily for linear low-density polyethylene (LLDPE) and low-density polyethylene (LDPE) blends. Research has shown that the addition of LDPE to LLDPE generally enhances the melt strength as a result of the long chain branching character of LDPE [9–11]. This increase in melt strength has been attributed to the immiscibility of the blend components [16, 17]. Increases in the melt strength of high-density polyethylene (HDPE)/LDPE blends have also been reported [9]. It has been suggested that the addition of metallocene catalyzed HDPE, which has small amounts of long chain branching, to metallocene-catalyzed LLDPE may provide better performance in blow molding, vacuum forming, and perhaps even film production [12].

Despite the abundance of recent studies on linear and branched PP blends, detailed investigations of their rheological and physical properties have been relatively scarce; those that have been undertaken have concentrated almost exclusively on the blends' rheology in extension. It has been commonly reported that the extensional rheology of these mixtures is highly sensitive to the presence of long chain branches [4, 7, 18]. Strain hardening behavior was observed, even at contents of branched PP as low as 10% [18]. Most of this work has examined blend formulations that are suitable for extrusion foaming.

This study aims to characterize in detail the rheological properties, phase behavior, and physical properties of linear and branched PP blends. Our work focuses on blends containing a high melt flow rate linear PP as part of an effort to develop a useful material that is suitable for injection foam molding applications.

EXPERIMENTAL

Materials

One linear and two branched PP samples supplied by Basell were used in this study; Pro-fax PD702 (LPP35) is an injection molding grade linear PP homopolymer. Pro-fax PF814 (BPP2.5) and PF611 (BPP30) are both high melt strength, branched homopolymer PP resins. The former is a foaming grade resin, whereas the latter is suitable for extrusion coating applications. All PPs used in this work have a density of 902 kg/m^3. The molecular weight and molecular weight distribution were measured using a Viscotek model 350 high temperature GPC, equipped with a dual angle LS (7° and 90°) viscometer and RI detectors. The properties of all polymers are summarized in Table 1.

A series of samples containing a range of branched PP compositions (LPP/BPP 20/80, 40/60, 60/40, and 80/20 by weight) were prepared, as outlined in the Blend Preparation section. All three pure PP samples were subjected to the same processing history in order to serve as control samples.

Blend Preparation

All blend components were dry-blended with 0.2% antioxidant (Irganox B225 from CibaGeigy). The dry blended formulations were then compounded at 210°C using a Haake Polylab Rheocord torque rheometer equipped with a Rheomix 610p mixing chamber and roller rotors until the torque profile exhibited steady state behavior (~6–7 min). The Haake was operated at ~70% capacity under nitrogen blanket to limit PP degradation.

Rheological Characterization

A Carver hydraulic press, heated at 200°C, was used to form compression molded discs that were ~2 mm in thickness and 25 mm in diameter. The samples were then characterized with a controlled stress rheometer (Visco-Tech by Rheologica) in the oscillatory mode using parallel plate fixtures 20 mm in diameter at a gap of 1.5 mm. All measurements were carried out under a nitrogen atmosphere to limit degradation and the absorption of moisture. Time sweeps confirmed that the samples were sufficiently stabilized and did not degrade during the duration of a typical experiment.

Strain sweeps were performed to ensure the measurements were within the linear viscoelastic (LVE) regime. The elastic modulus (G'), viscous modulus (G''), and complex viscosity (η^*) were measured as a function of the angular frequency (ω) at frequencies ranging from 0.04 to 188.5 rad/s. The rheological characterization of blends consisting of LPP35/BPP2.5 was done at 210°C in an effort to obtain data approaching the region of terminal flow, whereas the blends consisting of the low-viscosity components with LPP35 and BPP30 were measured at 180°C, to improve the accuracy of the measurement at low frequencies, given the low viscosity of the components. To further verify the accuracy of our low-frequency measurements and to determine the zero shear viscosity, creep experiments were performed at stresses between 2 and 5 MPa using the same controlled stress rheometer.

To characterize the blends at higher shear rates (20–2000 s^{-1}), a twin bore capillary rheometer RH2000 (Bohlin Instruments) was used at 210°C. The shear viscosities were calculated by applying the Bagley and Rabinowitch corrections [19].

Finally, the blends were rheologically characterized in simple extension using an SER Universal Testing Platform [20, 21] from Xpansion Instruments. As described by Sentmanat [22], the SER unit is a dual windup extensional rheometer that has been specifically designed for use as a detachable fixture on a variety of commercially available rotational rheometer host platforms. The particular SER model used in this study was designed for use on a VOR Bohlin rotational rheometer host system.

Specimens were prepared by compression molding the polymer samples between polyester films to a gage of

TABLE 1. Material properties.

Material	Trade name	MFR (g/10 min, 230°C)	M_n (kg/mol)	M_w/M_n
LPP35 (linear PP)	"Pro-fax" PD702	35	36.7	8.4
BPP2.5 (branched PP)	"Pro-fax" PF814	2.5	190	6.2
BPP30 (branched PP)	"Pro-fax" PF611	30	77.5	6.6

about 1 mm using a hydraulic press. Individual polymer specimens were then cut to a width of 6.4–12.7 mm. Typical SER extensional melt rheology specimens range from 40 to 150 mg in mass.

Measurements were conducted at 175°C, slightly above the melting point of the polymers, to ensure that the viscosities of the samples were high enough to prevent sagging. LVE oscillatory measurements were also obtained at 175°C using the VOR Bohlin rotational rheometer, to calculate the LVE shear stress growth plot.

Thermal Properties

A TA instrument differential scanning calorimeter (DSC) Q100 was employed to characterize the thermal properties of the blends. Approximately 5–8 mg of the samples were weighed and sealed in an aluminum hermetic pan, and subsequently heated from 30 to 200°C at a rate of 5°C/min. They were then held isothermally for 10 min to destroy any residual nuclei before cooling at 5°C/min. The melting temperatures and heats of fusion were obtained from a second heating sequence, performed at 5°C/min.

Mechanical Properties

An Instron 3369 universal testing machine was used to determine the tensile properties of all the materials. Measurements were carried out according to the ASTM D638 standard using Type V specimens stamped out from compression molded sheets prepared at 210°C. Five replicate runs at a crosshead speed of 10 mm/min were completed at each composition to ensure the reproducibility of the results.

Flexural tests were also performed using the Instron 3369, in accordance with ASTM D790, Procedure B, at a strain rate of 0.10 mm mm^{-1} min^{-1}. The samples having dimensions 127 × 12.7 × 3.2 mm^3 were compression molded at 210°C with the hydraulic press. The flexural modulus as well as flexural stresses and strains were calculated from the resulting curves.

RESULTS AND DISCUSSION

Oscillatory Shear Rheology

Figures 1 and 2 summarize the complex viscosities (η^*) and elastic moduli (G') of the LPP35/BPP30 and LPP35/BPP2.5 blends, respectively, as a function of frequency (ω). In both sets of blends, increasing the branched PP content results in higher complex viscosities and higher values of the elastic moduli at the low frequency range.
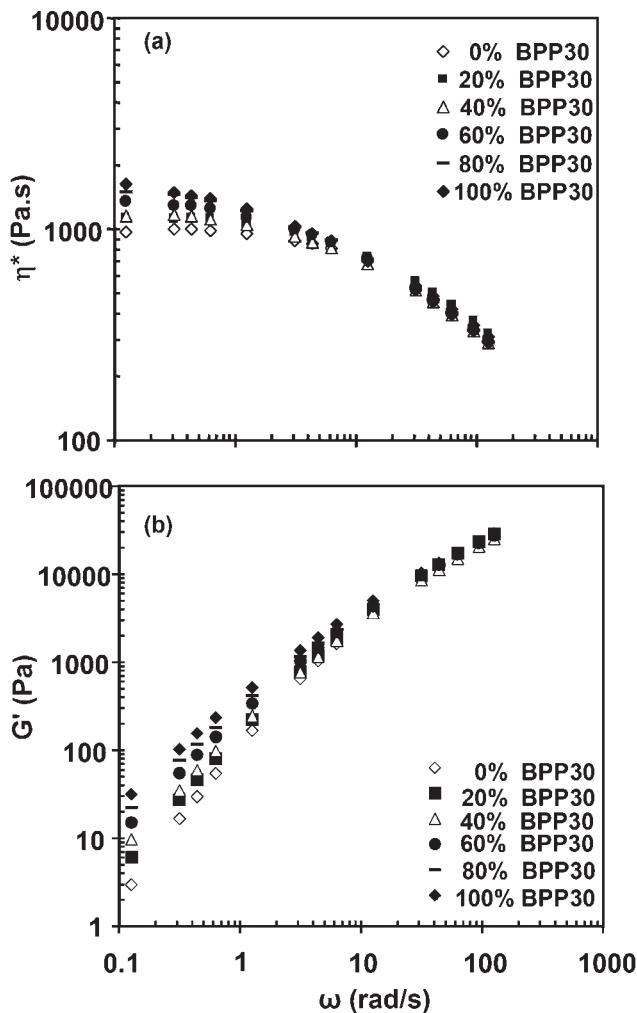

FIG. 1. (a) Complex viscosities, η^* and (b) elastic moduli, G', as a function of frequency, ω, for LPP35/BPP30 blends at 180°C.

The Cross model, *Eq. 1*, was applied to the data

$$\eta^*(\omega) = \frac{\eta_o}{1 + |\lambda\omega|^{(1-n)}} \tag{1}$$

where η^* is the complex viscosity; η_o is the zero shear viscosity; λ is a relaxation time; n is a constant related to the shear-thinning behavior; and ω is the frequency in rad/s. According to the Cross model parameters shown in Table 2, increasing the amount of branched PP in the blend results in higher zero shear viscosities and increased relaxation times. The zero shear viscosities, estimated using the Cross model, are plotted as a function of the blend composition in Fig. 3. These are in good agreement with the zero shear viscosities determined from the creep experiments, also included in Fig. 3. Both blend systems obey closely the log-additivity rule of viscosity in the melt state. Adherence to the additivity rule has been used as evidence of miscibility of the blend components in the melt state [13].

In a further effort to assess whether these blends are miscible, Cole–Cole plots [23] were constructed. Blends
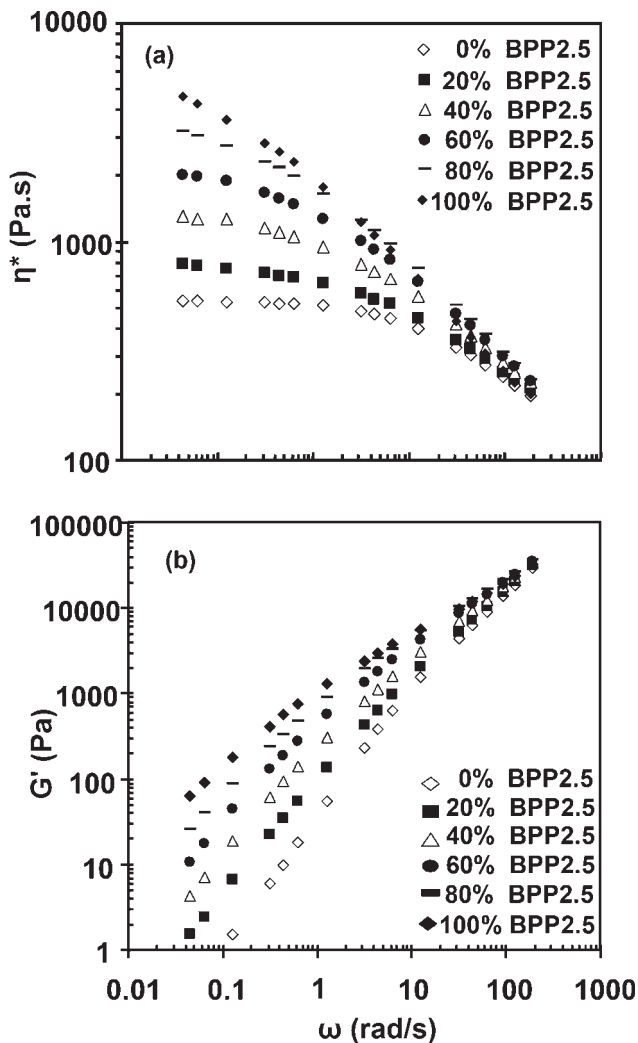
FIG. 2. (a) Complex viscosities, η^* and (b) elastic moduli, G', as a function of frequency, ω, for LPP35/BPP2.5 blends at 210°C.

TABLE 2. Cross and power law model parameters for LPP35/BPP30 and LPP35/BPP2.5 blends.

	Cross		Power law	
	η_0 (Pa s)	λ (s)	m (Pa s^n)	n
LPP35/BPP2.5[a]				
100/0	550	0.02	1589	0.54
80/20	835	0.06	2246	0.51
60/40	1493	0.25	2426	0.50
40/60	2430	0.64	2888	0.48
20/80	4076	1.71	2844	0.49
0/100	7451	8.38	4212	0.44
LPP35/BPP35[b]				
100/0	1020	0.02	1589	0.54
80/20	1170	0.04	1695	0.54
60/40	1226	0.06	1787	0.52
40/60	1452	0.08	1722	0.53
20/80	1566	0.14	1837	0.51
0/100	1767	0.21	1735	0.51

[a] From measurements obtained at 210°C.
[b] Cross model and power-law model parameters from measurements obtained at 180 and 210°C, respectively.

The weighted relaxation spectra, $(\lambda H(\lambda))$ as a function of $\log\lambda$ of the LPP35/BPP30 blends can be seen in Fig. 5. All the pure components and blend compositions exhibited single peaks; the characteristic relaxation time corresponding to BPP30 was approximately one order of magnitude higher than that of LPP35. Broader relaxation spectra, with higher characteristic relaxation times are expected because of the presence of branching [27, 28]. The smooth transition from the peak of the pure linear PP to the peak of the pure branched PP implies the miscibility of the LPP35/BPP30 blend components. Because of its substantially higher molecular weight, BPP2.5 displays a characteristic relaxation time that is orders of magnitude

that produce Cole–Cole plots with a semicircular shape are generally considered miscible [9, 14, 24]. Semicircular shapes are evident in Fig. 4a for the LPP35/BPP30 blends and in Fig. 4b at low BPP2.5 contents. The results are not conclusive in the case of the BPP2.5-rich LPP35/BPP2.5 blends, given that the terminal flow regime was not reached within the experimentally accessible range of frequencies (Fig. 4b).

Weighted relaxation spectra were constructed to extract further information about miscibility of these materials in the melt state [8, 25]. The continuous relaxation spectrum, $H(\lambda)$, was determined by fitting experimental $G'(\omega)$ and $G''(\omega)$ data in accordance with the numerical differentiation procedure developed by Ninomiya and Ferry using Eqs. 2 and 3 [26]

$$G'(\omega) = \int_{-\infty}^{\infty} H(\lambda) \frac{\omega^2 \lambda^2}{1 + \omega^2 \lambda^2} d\ln\lambda \qquad (2)$$

$$G''(\omega) = \int_{-\infty}^{\infty} H(\lambda) \frac{\omega\lambda}{1 + \omega^2 \lambda^2} d\ln\lambda. \qquad (3)$$
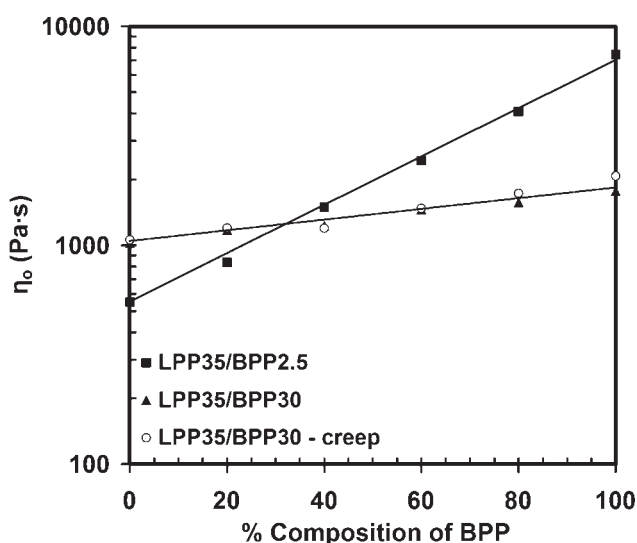

FIG. 3. Zero shear viscosity of LPP35/BPP2.5 and LPP35/BPP30 blends at 210 and 180°C, respectively. Solid lines denote the log-additivity rule of viscosity.
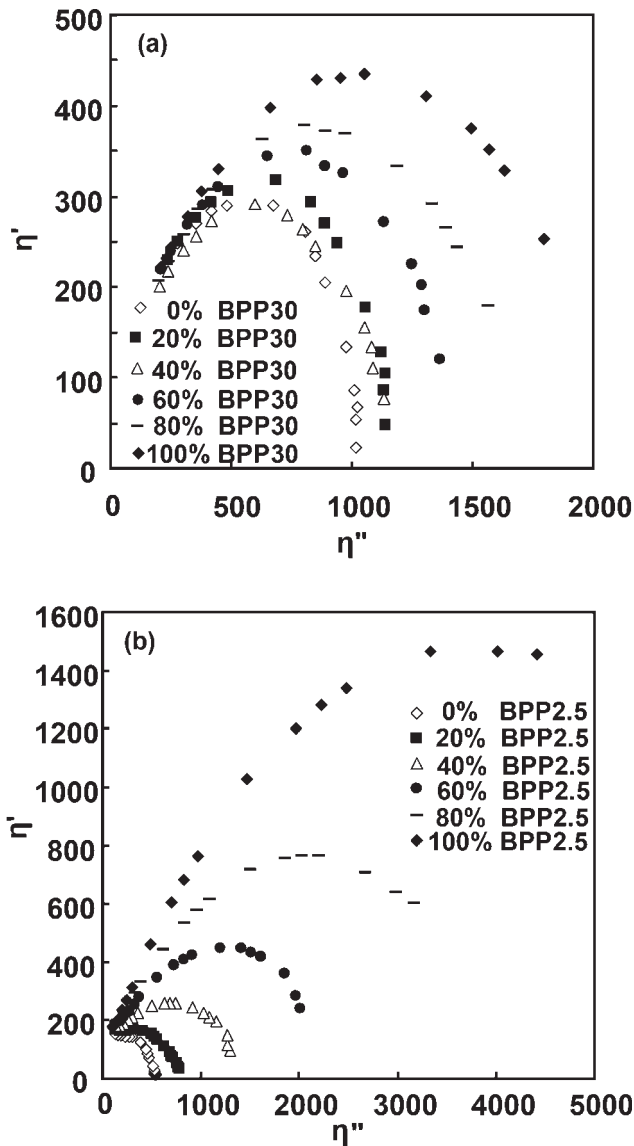
FIG. 4. Cole–Cole plots of (a) LPP35/BPP30 blends at 180°C, (b) LPP35/BPP2.5 blends at 210°C.

higher than that of LPP35. Given that the BPP2.5, as well as the BPP2.5-rich blends did not reach the terminal flow region, the relaxation spectra of this set of blends were not meaningful.

Steady Shear Rheology

Figure 6a and b illustrates the shear viscosities of the LPP35/BPP2.5 and LPP35/BPP30 blends, respectively, as a function of the shear rate. These superimpose well with complex viscosity versus frequency data, obtained from oscillatory experiments at the same temperature, indicating that these blends generally obey the Cox–Merz rule. It should be noted that a slight deviation from the Cox–Merz rule is observed for BPP2.5.

The power law model (*Eq. 4*), where *m* is the consistency index and *n* is the power-law index was applied to

the capillary data. The resulting parameters are summarized in Table 2.

$$\eta = m \, \dot{\gamma}^{n-1} \qquad (4)$$

The properties of LPP35 remain largely unaffected by the addition of BPP30. BPP2.5 has higher viscosity than LPP35 at low shear rates and displays pronounced shear thinning characteristics, because of the presence of long chain branching. The viscosities of the LPP35/BPP2.5 blends are intermediate to those of the pure components.

Extensional Rheology

Measurements of the tensile stress growth coefficients versus time, shown in Fig. 7a and b, provide a characterization of the extensional melt flow behavior of the two series of PP blends. Superimposed with the tensile growth curves in these figures is the LVE shear stress growth plot of $3\eta^+(t)$, which was obtained by using the LVE moduli to determine the relaxation spectrum in terms of a discrete spectrum of Maxwell relaxation times. The storage and loss moduli with respect to the discrete Maxwellian spectrum can be expressed as:

$$G'(\omega) = \sum_{i=1}^{N} G_i \frac{(\omega \lambda_i)^2}{1 + (\omega \lambda_i)^2} \qquad (5a)$$

$$G''(\omega) = \sum_{i=1}^{N} G_i \frac{\omega \lambda_i}{1 + (\omega \lambda_i)^2} \qquad (5b)$$

where ω is the frequency of oscillation and G_i and λ_i are the generalized Maxwell model parameters. The parameters (G_i, λ_i) of *Eq. 5* were determined using a nonlinear optimization program following the algorithm developed by Baumgartel and Winter [29]. Employing this program
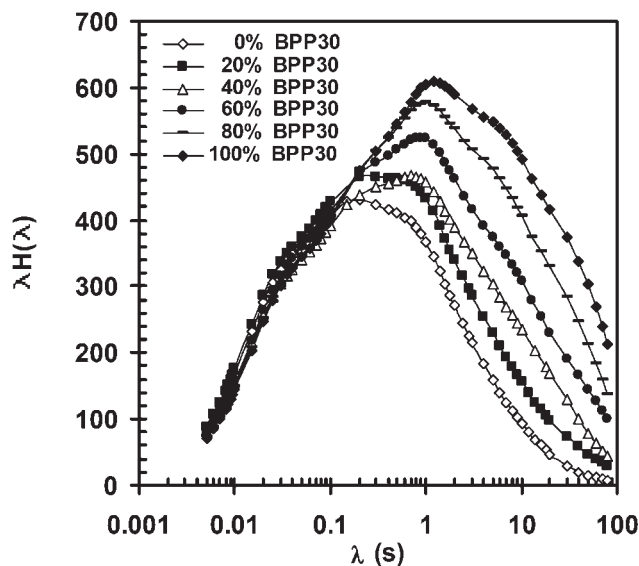

FIG. 5. Weighted relaxation spectra of LPP35/BPP30 blends at 180°C.
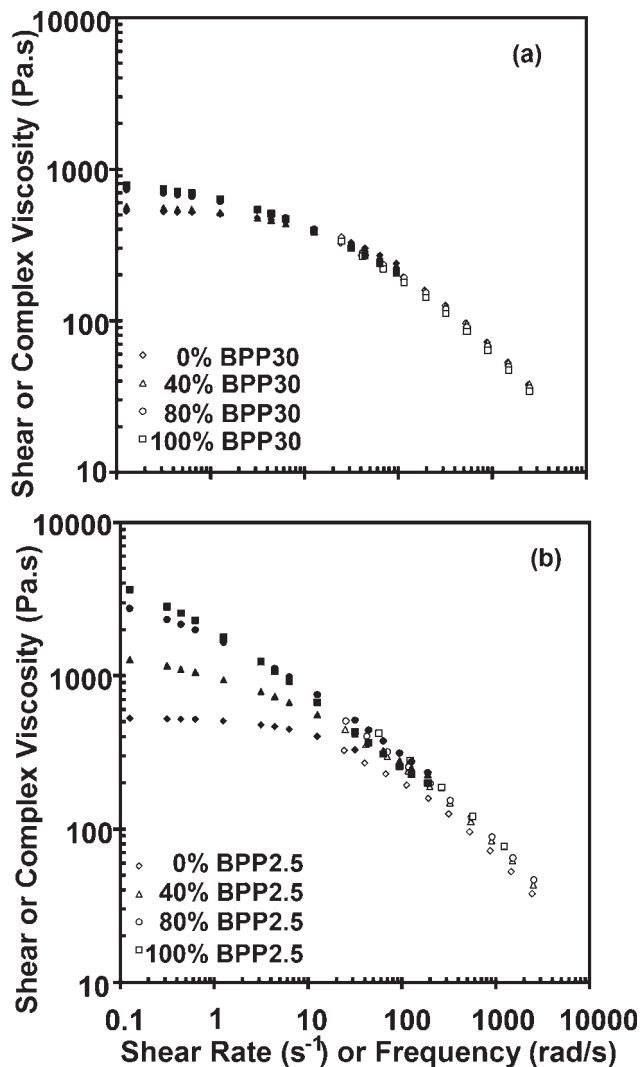
FIG. 6. Combined shear and complex viscosities as a function of shear rate or frequency at 210°C; (a) LPP35/BPP30 blends; (b) LPP35/BPP2.5 blends. Open symbols denote capillary data, whereas closed symbols represent oscillatory data.

results in the calculation of the least number of (G_i, λ_i) parameters (Parsimonious spectra). The discrete relaxation spectra of (G_i, λ_i) are then used in the following expression:

$$\eta_E^+ = 3\eta^+ = 3 \sum_i \frac{G_i}{\lambda_i} \left[1 - \exp\left(-\frac{t}{\lambda_i}\right) \right] \qquad (6)$$

For the linear PP, the agreement of the low-strain tensile portions of the tensile stress growth curves with the shear stress growth plots shown in Fig. 7a and b provides an experimental validation of Trouton's law, that is the ratio of extensional to shear viscosity was equal to 3. The higher plateau viscosity corresponding to $3\eta^+$ for the linear polymer provides additional evidence of the linearity of the molecules.

Branched PPs display strain hardening, manifested as a deviation from the predicted LVE stress growth behavior,

as expected in long chain branched polyolefins [7, 19, 28, 30, 31]. Significant strain hardening takes place even upon addition of low amounts of branched PP in linear PP, for both series of blends. This behavior becomes more pronounced as the Hencky strain rate is increased. First the tensile stress growth coefficient rises to higher levels as the amount of the long chain branched PP increases. The sudden decrease taking place subsequently corresponds to failure of the sample. The stress growth coefficient deviates from its linear behavior at earlier times when the amount of branched PP in the blend is augmented. Similar enhancements in strain hardening have been reported before in PE blends [9–11], as well as linear/branched PP blends [7, 18]. Micic et al. [16] attributed the observed enhancements in melt strength, extensional viscosity, and strain hardening of LLDPE/LDPE blends to the immiscibility of the blend components in the melt state. The influence of phase structure on the extensional properties of polyolefin blends has not been addressed extensively
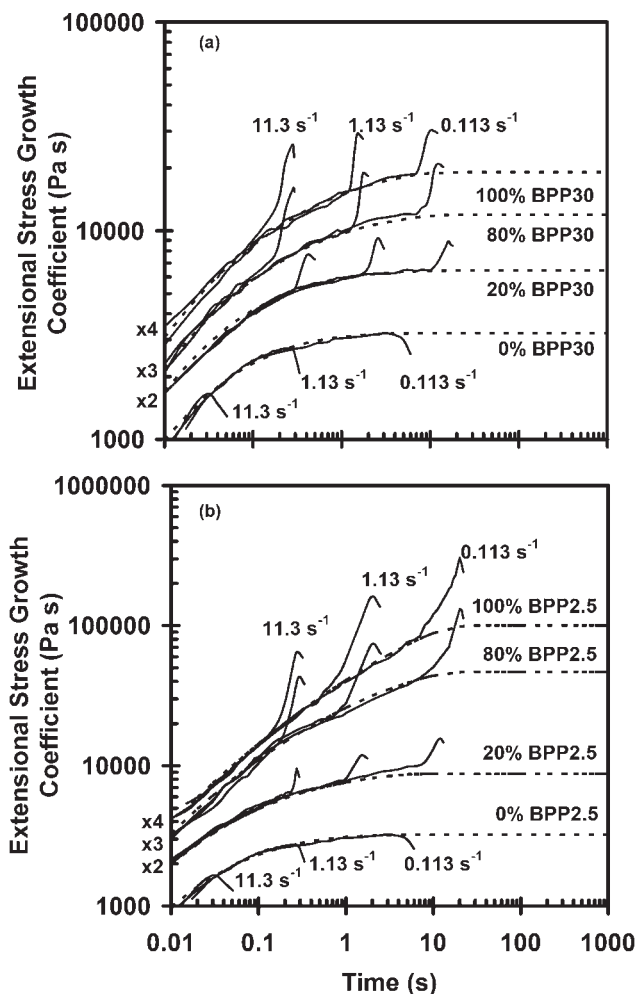

FIG. 7. Extensional stress growth coefficient rate at 175°C; (a) LPP35/BPP30 blends; (b) LPP35/BPP2.5 blends. Dotted lines denote the LVE shear stress growth coefficient $3\eta^+$ obtained from a Maxwell model fit, using experimental data obtained from linear oscillatory measurements at 175°C.

TABLE 3. Thermal and tensile properties for LPP35/BPP30 and LPP35/BPP2.5 blends.

	T_m	T_c	Crystallinity (%)	Strain at yield	Stress at yield	Young's modulus (MPa)
LPP35/BPP30						
100/0	165.9	111.4	60.7	29.0 ± 1.6	30.2 ± 1.9	327.4 ± 41.9
80/20	163.5	126.0	59.5	22.5 ± 0.6	33.6 ± 0.1	406.3 ± 49.7
60/40	163.9	127.9	60.3	18.6 ± 1.7	35.9 ± 1.2	443.3 ± 19.6
40/60	163.6	127.5	64.9	20.0 ± 0.5	34.9 ± 0.5	415.3 ± 22.7
20/80	163.9	128.5	61.7	22.1 ± 0.1	36.5 ± 0.1	424.0 ± 30.5
0/100	164.1	128.6	62.8	19.1 ± 1.6	36.9 ± 1.9	456.1 ± 43.1
LPP35/BPP2.5						
100/0	165.9	111.4	60.7	29.0 ± 1.6	30.2 ± 1.9	327.4 ± 41.9
80/20	164.1	128.8	53.7	29.9 ± 0.5	29.1 ± 1.1	253.0 ± 0.1
60/40	163.3	129.6	56.7	27.4 ± 1.4	30.6 ± 0.1	307.4 ± 20.8
40/60	162.8	130.1	54.0	23.2 ± 2.5	33.9 ± 0.1	373.4 ± 34.0
20/80	162.0	129.8	52.8	23.1 ± 1.7	33.5 ± 0.5	393.1 ± 8.8
0/100	161.3	129.0	43.2	24.6 ± 1.6	33.5 ± 0.5	374.9 ± 17.5

in the literature, but the results of the present study suggest that miscible PP blends exhibit strain hardening.

Thermal Properties

All sets of blends exhibit single melting and crystallization peaks. The melting and crystallization points (T_m and T_c, respectively) and crystallinities for both sets of blends are summarized in Table 3. The melting points of LPP35/BPP2.5 blends have an almost linear dependence on the composition of the branched PP, with the melting point decreasing as BPP2.5 content increases. This provides further evidence of miscibility of these blends. Substantial decreases in crystallinity are also noted, with BPP2.5 having a significantly lower crystallinity than the linear PP. These observations are obviously because of the disruption of the crystalline structure of PP in the presence of long chain branching.

The melting points of the LPP35/BPP30 remain virtually unaffected and addition of BPP30 to the blends yields a slight increase in crystallinity. This result was unexpected and it may be because of BPP30 containing lower amounts of long chain branching than BPP2.5 and/or having a more homogeneous long chain branching distribution.

With respect to the crystallization temperatures, both sets of blends show a dramatic increase upon the addition of a small fraction of branched PP; further additions caused only minimal changes. This trend is similar to previously published results [5].

Mechanical Properties

Table 3 displays the tensile properties, including the strain at yield (%), the stress at yield (MPa), and the Young's moduli. For both sets of blends, increasing the branched PP content leads to increased tensile stress and Young's modulus, and decreased tensile strain.
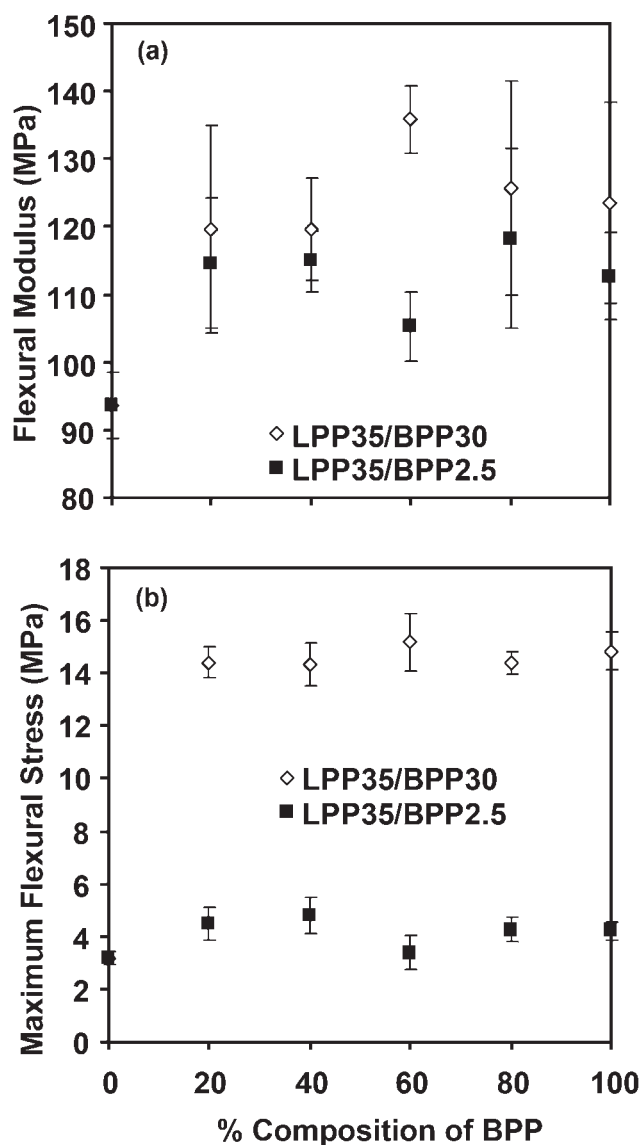

FIG. 8. (a) Flexural moduli and (b) flexural stresses as a function of BPP content for LPP35/BPP2.5 and LPP35/BPP30 blends.

Flexural properties, including maximum flexural stress and flexural modulus as a function of blend composition, can be seen in Fig. 8. The flexural moduli of all blends are higher than the linear sample; however, the increase is much more pronounced in the blends containing BPP30.

Overall, all blends exhibit better stiffness than the linear PP. Additionally, the LPP35/BPP30 blends demonstrate better flexural and tensile properties when compared with the LPP35/BPP2.5 system. This trend may be attributed to the higher values of crystallinity exhibited by the LPP35/BPP30 blends.

CONCLUSIONS

Blends of linear and branched PPs exhibited increased melt elasticity and strain hardening, and produced more pronounced shear thinning behavior. Based on the rheological and thermal characterization, these blends appeared to be miscible.

The melting points and crystallinities were affected substantially upon introduction of the higher molecular weight BPP2.5 resin, whereas remained virtually unaffected in the presence of BPP30. The crystallization points increased significantly upon addition of low amounts of branched PPs for both sets of blends.

The flexural properties and tensile moduli increased with the introduction of branched PP; the blends containing BPP30 displayed better mechanical properties, and this was credited to the higher crystallinity of BPP30.

ACKNOWLEDGMENTS

REFERENCES

1. P. Spitael, C.W. Macosko, and A. Sahnounne, *Proc. SPE ANTEC*, **2**, 1791 (2002).

2. G.J. Nam, J.H. Yoo, and J.W. Lee, *J. Appl. Polym. Sci.*, **96**, 1793 (2005).

3. H.E. Naguib, C.B. Park, U. Panzer, and N. Reichelt, *Polym. Eng. Sci.*, **42**, 1481 (2002).

4. A.D. Gotsis, B.L.F. Zeevenhoven, and A.H. Hogt, *Polym. Eng. Sci.*, **44**, 973 (2004).

5. H.E. Naguib, J.X. Xu, C.B. Park, A. Hesse, U. Panzer, and N. Reichelt, *Proc. SPE ANTEC*, **2**, 1623 (2001).

6. N. Reichelt, M. Stadlbauer, R. Folland, C.B. Park, and J. Wang, *Cell. Polym.*, **22**, 315 (2003).

7. P. Spitael and C.W. Macosko, *Polym. Eng. Sci.*, **44**, 2090 (2004).

8. Y. Fang, P.J. Carreau, and P.G. Lafleur, *Polym. Eng. Sci.*, **45**, 1254 (2005).

9. K. Cho, B.H. Lee, K.-M. Hwang, H. Lee, and S. Choe, *Polym. Eng. Sci.*, **38**, 1969 (1998).

10. P. Micic, S.N. Bhattacharya, and G. Field, *Intern. Polym. Process.*, **XI**, 14 (1996).

11. A. Ghijsels, J.J.S.M. Ente, and J. Raadsen, *Intern. Polym. Process.*, **VII**, 44 (1992).

12. C. Liu, J. Wang, and J. He, *Polymer*, **43**, 3811 (2002).

13. L.A. Utracki and B. Schlund, *Polym. Eng. Sci.*, **27**, 512 (1987).

14. H. Kwag, D. Rana, K. Cho, J. Rhee, T. Woo, B.H. Lee, and S. Choe, *Polym. Eng. Sci.*, **40**, 1672 (2000).

15. F. Chen, R. Shanks, and G. Amarasinghe, *J. Appl. Polym. Sci.*, **81**, 2227 (2001).

16. P. Micic, S.N. Bhattacharya, and G. Field, *Intern. Polym. Process.*, **XII**, 110 (1997).

17. P. Micic, S.N. Bhattacharya, and G. Field, *Intern. Polym. Process.*, **XIII**, 50 (1998).

18. J. Stange, C. Uhl, and H. Münstedt, *J. Rheol.*, **49**, 1059 (2005).

19. J.M. Dealy and K.F. Wissbrum, *Melt Rheology and Its Role in Plastics Processing*, Kluwer, Boston (1999).

20. M.L. Sentmanat, U.S. Patent 6, 578, 413 (2003).

21. M.L. Sentmanat, *Rheol. Acta*, **44**, 657 (2003).

22. M.L. Sentmanat, E.B. Muliawan, and S.G. Hatzikiriakos, *Rheol. Acta*, **44**, 1 (2004).

23. K.S. Cole and R.H. Cole, *J. Chem. Phys.*, **9**, 341 (1941).

24. L.A. Utracki, in *Two Phase Polymer Systems*, L.A. Utracki, Ed., Hanser Publishers, New York (1991).

25. C. Lacroix, M. Aressy, and P.J. Carreau, *Rheol. Acta*, **36**, 416 (1997).

26. J.D. Ferry, *Viscoelastic Properties of Polymers*, 3rd ed., Wiley, New York (1980).

27. C. Tzoganakis, *Can. J. Chem. Eng.*, **72**, 749 (1994).

28. A.D. Gotsis, B.L.F. Zeevenhoven, and C. Tsenoglou, *J. Rheol.*, **48**, 895 (2004).

29. M. Baumgartel and H.H. Winter, *Rheol. Acta*, **28**, 511 (1989).

30. M.L. Sentmanat, B.N. Wang, and G.H. McKinley, *J. Rheol.*, **49**, 585 (2005).

31. S. Kurzbeck, F. Oster, H. Münstedt, T.Q. Nguyen, and R. Gensler. *J. Rheol.*, **43**, 359 (1999).